Italian Journal of Engineering Geology and Environment
www.ijege.uniroma1.it

MULTI-TEMPORAL ANALYSIS OF THE GEOMORPHIC EVOLUTION OF THE FAILURE SURFACE OF THE VAJONT LANDSLIDE

Davide DONATI[(*)], Alessandro LAMBERTINI[(*)], Doug STEAD[(**)], Monica GHIROTTI[(***)] & Lisa BORGATTI[(*)]

[(*)]Alma Mater Studiorum University of Bologna - Department of Civil, Chemical, Environmental and Materials Engineering - Bologna, Italy
[(**)]Simon Fraser University - Department of Earth Sciences - Burnaby, V5A 1S6, Canada
[(***)]University of Ferrara - Department of Physics and Earth Sciences - Ferrara, Italy.
Corresponding author: davide.donati17@unibo.it

EXTENDED ABSTRACT

I fenomeni franosi rappresentano uno dei georischi più significativi che caratterizzano l'ambiente montano. Se da un lato gli impatti delle singole frane sono in genere spazialmente limitate alle aree colpite o all'immediato intorno, in alcuni casi il verificarsi di eventi di particolare entità, caratterizzate da volumi di svariati milioni di metri cubi, possono causare impatti sociali, economici e ambientali talvolta particolarmente severi e duraturi. Nella maggioranza dei casi, questi eventi sono caratterizzati dal distacco improvviso di volumi significativi di ammasso roccioso, che determinano una notevole perturbazione nello stato tensionale e nella cinematica del versante interessato, di conseguenza, può emergere una condizione che avvicina all'equilibrio limite per la porzione di versante non coinvolta nel fenomeno franoso. Gli effetti di tale condizione possono essere molto variabili e possono determinare l'inizio di una evoluzione progressiva e graduale del versante, a causa del continuo distacco di materiale versante roccioso (crolli in roccia) che può protrarsi nel lungo periodo e, talvolta, il distacco di altre frane significative, volumetricamente simili al primo evento, determinando eventi multi-stage.

In questo lavoro gli autori descrivono un'analisi dell'evoluzione morfologica che ha caratterizzato una parte della superficie di scivolamento della grande frana del Vajont del 1963, una delle più famose e distruttive frane registrate a livello mondiale. I cambiamenti e l'evoluzione della superficie di distacco della frana alle pendici del Monte Toc vengono investigate, per il periodo 2017-2023, utilizzando una combinazione di dataset bi- e tri-dimensionali. Lo studio si fonda su un'analisi di change detection che viene condotta utilizzando nuvole di punti derivanti da rilievi laser scanner aerei. Il primo dataset è messo a disposizione dalla Regione Friuli Venezia-Giulia tramite il relativo geoportale online (EagleFVG), e rappresenta lo stato dell'area al 2017, anno in cui il rilievo è stato effettuato, sotto forma di nuvola di punti. Il secondo dataset deriva da un rilievo condotto attraverso l'utilizzo di un drone equipaggiato con sensore laser scanner, che ha permesso di ottenere le nuvole di punti di due aree nei lobi occidentale ed orientale della superficie di scivolamento della frana. Il confronto, effettuato utilizzando il tool M3C2 all'interno del software CloudCompare, ha permesso di individuare le aree ove distacchi si sono verificati nel periodo analizzato, nonché di procedere a una stima della superficie e volume dei blocchi coinvolti. Le stesse aree sono state analizzate utilizzando fotografie ad alta risoluzione raccolte dagli autori nel corso di attività di campagna condotte nel corso degli ultimi 20-30 anni. Il confronto e la combinazione dei risultati delle analisi bi- e tri-dimensionali hanno permesso di verificare le caratteristiche e la conformazione dei blocchi prima e dopo il distacco, ed evidenziare il ruolo di discontinuità preesistenti e fenomeni di rottura fragile sull'evoluzione del versante.

Il presente contributo rappresenta il primo passo di una ricerca che punta ad investigare il comportamento e la stabilità residua di versanti in roccia a seguito di frane significative in termini di volume. I prossimi step della ricerca includeranno la pianificazione e l'attuazione di un rilievo laser scanner via drone dell'intera superficie di scivolamento e del deposito della frana del Vajont, ottenendone un modello tri-dimensionale aggiornato. Questo sarà utilizzato, assieme a modelli fotogrammetrici derivanti da Structure-from-Motion e fotografie terrestri ed aeree, a ricostruire l'evoluzione del versante dopo il distacco della frana del 1963, evidenziando al contempo i fattori geologici e strutturali più importanti nel controllo dell'evoluzione post-frana di versanti in roccia.

IJEGE, Special Issue 1 (2024): 105-113, DOI: 10.4408/IJEGE.2024-01.S-12
E-ISSN 2035-5688 | ISSN 1825-6635 /

ABSTRACT

Landslides are among the most common type of hazard that affect mountainous regions. While the impact of the single landslide is often localized and limited to the influence area, in some cases, the occurrence of major events can result in significant and long-lasting social, economic, and environmental impacts that extend beyond the area directly affected by the event. These major landslides involve the sudden detachment of large volumes of rock mass and cause significant disturbance of in-situ stress field due to slope debuttressing and reduction in lateral support, which often result in conditions of limit equilibrium affecting the remaining part of the slope. Effects of such limit equilibrium conditions can range from a long term, gradual morphological evolution of the slope due to progressive detachment of material, to the development of multi-stage landslides, involving the failure of volumes of rock mass similar in magnitude and impacts to the original event.

In this work, we investigate the post-failure morphological evolution of the daylighting rupture surface and deposit of one of the most important historical landslides, the 1963 Vajont Slide. A preliminary investigation of a pair of airborne laser scanner (ALS) datasets, collected in 2017 and 2023, is undertaken to assess and compute the change in elevation across selected areas within the rupture surface. Based on a three-dimensional change detection analysis, the observed volumetric changes of selected, inferred rockfall events are estimated. Terrestrial and airborne photographs are also used to identify the unstable volumes that have progressively detached, as well as the damage features that outlined these unstable blocks. Finally, we discuss the long-term evolution of the slope with focus on progressive damage accumulation and its spatial relationship with inherited, tectonic structures.

Ultimately, this contribution is intended to highlight the important role of post-slope failure damage accumulation on the long-term stability of rock slopes, emphasizing the critical role that post-failure monitoring and analysis can play in outlining the residual landslide hazard and, in some instances, the potential development of multi-stage landslides.

***Keywords**: Vajont Slide, remote sensing, slope damage, multi-temporal analysis.*

INTRODUCTION

The occurrence of landslide events is often accompanied by the detachment of volumes of material from the slope both prior to and after the major event. In all cases, pre-failure detachment of material is limited compared to the main event, and often occurs as a series of rockfalls that prepare the slope for failure by progressively increasing the overall kinematic freedom of the unstable mass (Kromer *et alii*, 2015; Donati *et alii*, 2023). In contrast, the post-failure behavior of a rock slope can vary greatly due to numerous factors including slope morphology, degree of rock mass fracturing, stress, and environmental conditions such as lack of vegetation cover, temperature cycles, and others. In some cases, the impact of the failure on slope kinematics and lateral support is significant enough to cause or facilitate subsequent major instabilities that can post-date the initial event by periods of time, ranging from days (*e.g.*, Willenberg *et alii*, 2008; Friele *et alii*, 2020) to centuries and beyond (*e.g.*, Donati *et alii*, 2023). In most cases, however, residual instability conditions arise, which, similar to pre-failure conditions, entail detachment of rockfalls that may continue for varying lengths of time before the slope attains a new condition of geomorphic or kinematic equilibrium. In those areas where residual, post-failure rockfall activity may lead to an unacceptable risk to communities or infrastructure, mitigation activities can be undertaken to limit impacts or prevent further detachments (Wyllie, 2017).

Combined stress redistribution and evolution of slope kinematics (e.g., due to local changes in orientation and steepness) that may affect a rock slope after a failure can also increase the rate of rock mass damage accumulation, further promoting post-failure rockfall activity. Brittle fracture propagation may lead to the formation of fully persistent release surfaces along the boundaries of potentially unstable blocks (Donati *et alii*, 2023). The subsequent block detachment may reduce or completely remove lateral and/or basal support of adjacent blocks, causing further stress redistribution and additional brittle damage, potentially resulting in a migration of the instability.

A particular focus of recent published literature is on the occurrence of preparatory rockfall events (failure precursors). This has allowed the development of new approaches and methodologies for forecasting the time and extension of more significant rock slope failures (e.g., Rosser *et alii*, 2007; Kromer *et alii*, 2015; Walton *et alii*, 2023). Due to the inherently hazardous conditions that characterize unstable and potentially unstable rock slopes, and the need to monitor large areas at appropriate spatial and temporal resolutions, remote sensing techniques and datasets are increasingly exploited to investigate rockfall activity. In particular, terrestrial laser scanning (TLS) is now routinely employed for rockfall monitoring purposes, in view of the high dataset resolution and survey repeatability it can provide. To a lesser extent, digital photogrammetry and high-resolution photography are also employed, despite the inability to recover 3D information from a single station and the inability to collect data in conditions of limited visibility. As opposed to pre-failure rockfall monitoring, post-failure rockfall activity is seldom treated in the scientific literature, and its characterization and analysis appear to be largely undertaken by engineers and geoscientists tasked with slope stabilization and hazard and risk mitigation. As a result, the analysis of long-term, post-failure slope processes and brittle damage, responsible for the evolution of the slope in the aftermath of major failures, has been the subject of limited research.

This paper represents a preliminary step in addressing this research gap. In particular, the objective is to assess the potential application of remote sensing methods in the analysis of post-failure damage accumulation, and to investigate the potential role of damage in controlling rockfall activity following major landslides in rock slopes. To achieve this goal, we use a combination of multi-temporal ALS and long-range photography to investigate the post-failure evolution of the scar of the 1963 Vajont landslide.

THE 1963 VAJONT SLIDE

The Vajont slide is a 270 million m^3 rock slope failure that occurred on October 9th, 1963. The landslide was caused by the impoundment of a reservoir within the Vajont gorge, a tributary of the Piave River in northeastern Italy (Fig. 1a,b). The landslide, which had moved for several years before failure at rates of mm/day to cm/day, suddenly accelerated to a speed of about 100 km/hr, driving the water in the reservoir up to about 200 m up the north slope of the valley, pushing more than 30 million m^3 of water more than 100 m over the dam. The flood wave moved down the Vajont Gorge to the Piave River, where it destroyed many villages, and most of the town of Longarone, resulting in over 1,900 fatalities (Semenza & Ghirotti, 2000).

The landslide occurred in a relatively complex structural setting, which strongly controlled both the morphology of the area and its long-term evolution (Massironi *et alii*, 2013; Semenza & Ghirotti, 2000). The Erto syncline controls the location and direction of the Vajont Valley. The left side of the valley constitutes the southern limb of the syncline, which dips easterly and forms the long-recognized chair-shaped morphology of the Mount Toc (Fig. 1c), clearly visible from the Piave River valley and Longarone. The boundaries of the landslide are also controlled by geological structures. The eastern boundary of the landslide follows a sub-vertical scarp that constitutes the Col Tramontin Fault, whereas the upper and part of the western boundaries are controlled by the Col delle Erghene line. The location and orientation of the Massalezza gully follows the axis of a north-plunging syncline, which also separates the eastern and the western limbs of the Vajont Slide (Massironi *et alii*, 2013).

The geology of the region is characterized by the presence of Triassic to Paleocene calcareous formations. The geological formations in the area include the Dolomia Principale Formation (Upper Triassic), the Soverzene and Igne Formations (Liassic), the Vajont Limestone (Dogger), the Ammonitico Rosso, Fonzaso,

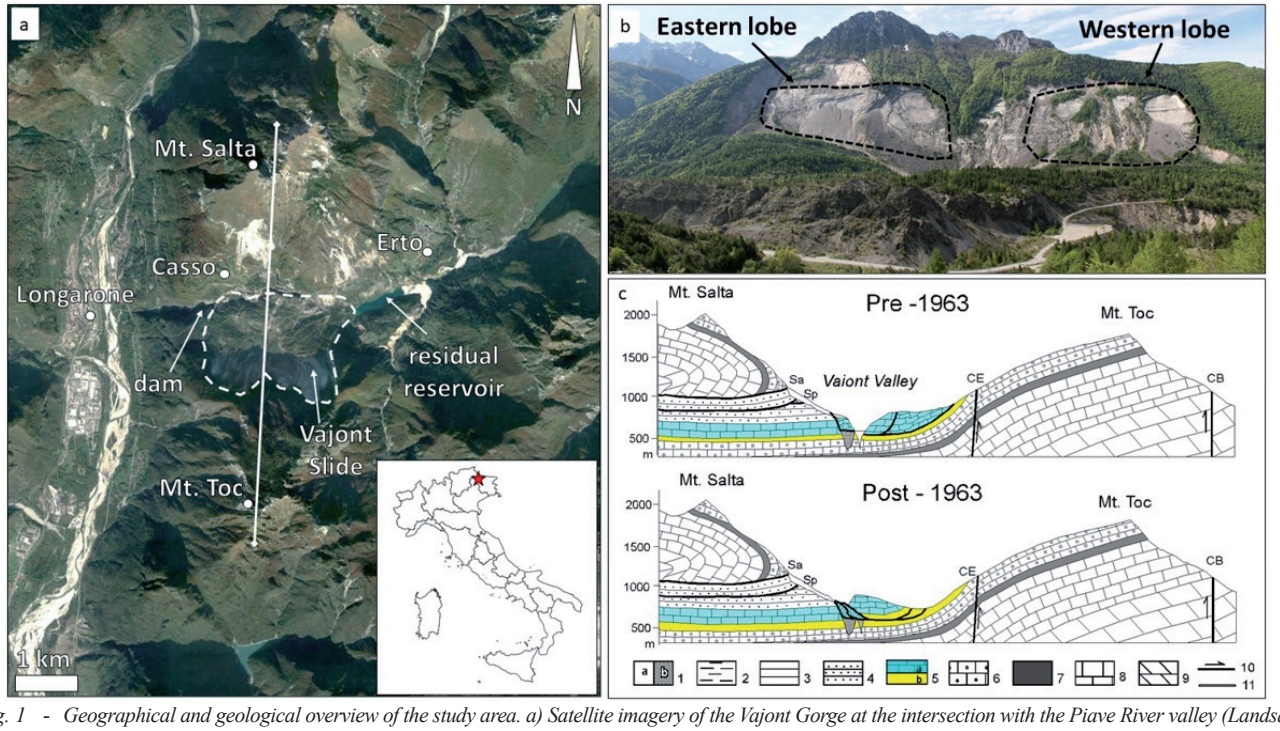

Fig. 1 - Geographical and geological overview of the study area. a) Satellite imagery of the Vajont Gorge at the intersection with the Piave River valley (Landsat/ Copernicus imagery). The dashed, white line marks the boundaries of the landslide area. The solid white line represents the trace of the profiles shown in tab c. The inset shows the location of the Vajont Slide in northern Italy. b) view of the scar and deposit of the Vajont Slide from the village of Casso, on the opposite side of the Vajont gorge. The dashed, black lines mark the areas investigated in this preliminary study, referred to as "Western lobe" and "Eastern lobe". c) Geological sections before and after the landslide along the profile shown in tab a. Formations involved in the landslides are colored in the section. Legend: 1: Quaternary (a), Alluvial gravels (b); 2: Flysch Fm. (Eocene); 3: Marls of Erto Fm. (Paleocene); 4: Scaglia Rossa Fm. (Upper Cretaceous–Lower Paleocene); 5: Socchér Limestone Fm. s.l. (a), Ammonitico Rosso and Fonzaso Fms. (Cretaceous–Jurassic) (b); 6: Vajont Limestone Fm. (Middle Jurassic); 7: Igne Fm. (Early Jurassic); 8: Soverzene Fm. (Middle Jurassic); 9: Dolomia Principale Fm. (Upper Triassic); 10: Faults and overthrusts; 11: Failure surface of the 1963 landslide; CE: Col delle Erghene Faul; CB: Croda Bianca Fault (from Ghirotti, 2012)

and Socchér Formations (Cretaceous-Jurassic) and Scaglia Rossa Formation (Upper Cretaceous-Lower Paleocene) (Fig. 1c). The displacement of the landslide occurred mainly along weak and thin clay layers (a few cm in thickness) that occur within the Fonzaso Formation (Hendron & Patton, 1987).

Studies conducted prior to the failure, most notably Giudici & Semenza (1960) provided evidence that the southern slope of the Vajont Gorge was formed by the deposit of a paleo-landslide that moved at some point in the past, filling the valley. These deposits were subsequently eroded and incised by the Vajont stream, resulting in the morphology that was visible prior to 1963. However, the characteristics of such a prehistoric slope movement remain the subject of debate (*e.g.*, Paronuzzi & Bolla, 2012; Wolter *et alii*, 2016).

Post-failure evolution of the landslide is generally limited to the outcropping failure surface, which has been affected by a continuous and progressive detachment of material, resulting in gradual increase in the elevation of the scree and talus deposits at the base of the slope. In the immediate aftermath of the failure (*i.e.*, within a few days) a cluster of depressions also formed in the western part of the deposit, near the dam, which was referred to as "Costa dei Crateri" (loosely translatable as Craters' Ridge) in Semenza (1965).

DATA AND METHODS

The analyses conducted in this research combine 2D and 3D dataset to investigate the geomorphic evolution of the scar of the Vajont Slide between 2017 and 2023.

The first part of the study focuses on the analysis of multi-temporal 3D datasets. In particular, we perform a change detection analysis using the ALS dataset that was made freely available by the Friuli Venezia-Giulia Region (surveyed in 2017) and a dataset collected in 2023 using an unmanned aerial vehicle (UAV) mounted with an ALS sensor. The 2023 dataset covers two areas along the outcropping failure surface, one located on the upper part of the western lobe, and the other one on the central part of the eastern lobe (Fig. 1b). The 2023 UAV flights represent a preliminary test that is being used to prepare a later survey that will be undertaken in 2024 to provide an updated 3D model of the whole landslide area (covering both the deposit and the failure surface). The UAV employed for the analysis is a DJI Matrice 300 RTK, equipped with a Zenmuse L1 LiDAR (light detection and ranging) sensor (Fig. 2).

The flight plan was defined using the DJI Pilot 2 app (DJI, 2023A), which includes a terrain following feature that allowed a flight elevation of 100 m above the ground level to be maintained during the survey. Flight height and speed were chosen to allow the creation of a raw point cloud with an average point density of 100 pts/m^2. Raw data processing was conducted using the software DJI Terra (DJI, 2023B), which allowed the point clouds to be exported in a LAS format. Point clouds were then imported in the

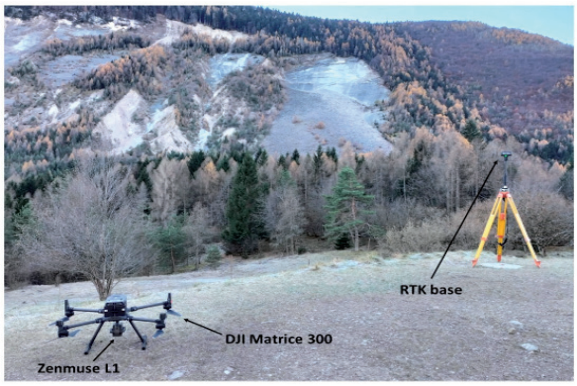

Fig. 2 - Photograph of the DJI Matrice 300 equipped with the Zenmuse L1 LiDAR sensor and the RTK base mounted on a surveyed ground control point (GCP)

open code CloudCompare (CloudCompare, 2022), where post-processing was conducted which included a) filtering laser pulse returns different from single and last pulses, b) noise removal from the point clouds, using built-in tools, c) subsampling of the cloud, resulting in an average point density of about 5-6 pts/m^2, similar to the to the existing 2017 ALS dataset, d) classification of the point cloud, after appropriate training, using the CANUPO classifier (Brodu & Lague, 2012). Overall, these steps decreased the number of points in the point clouds from approximately 170 million to 7.4 million for the eastern lobe cloud, and from 86 million to 6.7 million for the western lobe cloud. During post-processing, most of the vegetation was also virtually removed from the point clouds, providing a "bare earth" (BE) dataset. BE point clouds were then registered using the 2017 ALS dataset, and change detection performed using the M3C2 tool in CloudCompare (Lague *et alii*, 2013).

Within the paper, we also present and analyze historical photographs taken by the authors over the course of several visits to the site during the past three decades. In particular we use these photographs to identify the spatio-temporal characteristics of the rockfall source areas from a slope damage perspective.

As this analysis largely focuses on rockfall events sourcing from the outcropping failure surface, only the area where bedrock outcrops (*i.e.*, it is not covered by talus) have been investigated. The analysis was conducted by visual inspection of the photographs within those areas where a change was observed in the multi-temporal ALS analysis.

RESULTS AND DISCUSSION

The ALS change detection analysis, conducted using the 2017 and 2023 datasets, allowed for the identification of several blocks that failed generating rockfalls.

In the western lobe of the outcropping failure surface, three failed blocks were identified, referred to as Wb1, Wb2, and Wb3 in figure 3.

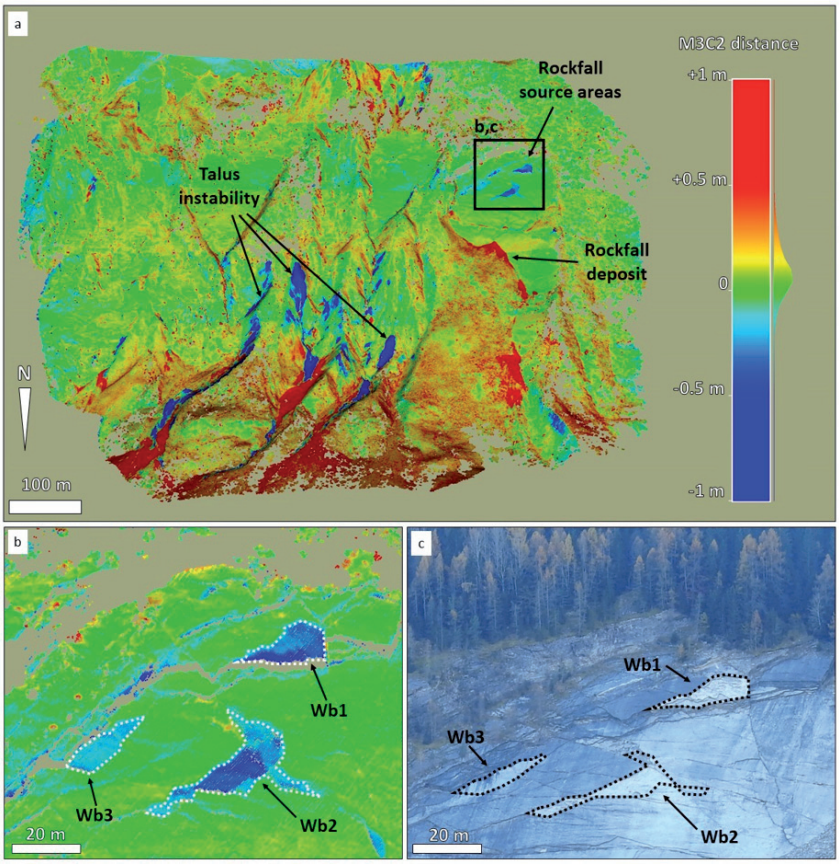

Fig. 3 - Overview of the results of the ALS change detection of the western lobe. Red and blue colors indicate gain and loss of material. Color scale has been trimmed at negative and positive changes of 1 m. a) General view of the investigated area. Note the material loss on the western part of the upper slope. b) detail of the area where blocks Wb1, Wb2, and Wb3 have been identified. Note the varying thickness of the block, which is likely controlled by bedding plane spacing. c) high-resolution photo of the same area, where the detached blocks are highlighted by the relatively lower surface alteration, compared to surrounding rock mass. In this sense, Wb1 area appears to be the most recent detachment, whereas Wb3 is the earliest one

All identified blocks are characterized by a tabular shape and appear to be bounded by discontinuities. Blocks are characterized by surface areas of 127 m^2 (Wb1), 347 m^2 (Wb2), and 122 m^2 (Wb3). The thickness of the blocks is likely controlled by the spacing of bedding planes and varies between 15-25 cm (Wb3) and 30-40 cm (Wb1). The thickness of block Wb2 is spatially variable. The upper part and the western side of block Wb2 are 15-25 cm in thickness, whereas the remaining part of the block is 30-40 cm thick, locally reaching up to 50 cm in thickness. The block volumes can be estimated as 40 m^3 for Wb1, 105 m^3 for Wb2 and 30 m^3 for Wb3.

The deposit area for the described rockfalls is represented by the talus cone immediately below, the apex of which gained 6 m in elevation, partly covering the lower part of the outcropping failure surface.

The eastern lobe of the rupture surface is significantly more tectonically disturbed than the rest of the failure surface. Intense multi-order folding that characterizes the area generated the structural terrace that cuts obliquely across the eastern lobe (Massironi *et alii*, 2013) and promote a more intense rock mass fracturing compared to the western lobe.

The eastern lobe also shows significant rockfall activity, involving a large volume of material in at least one case (Fig. 4). In particular, a major failure was registered in February 2021, which caused the detachment of a 5-6 m thick rock slab from the easternmost part of the landslide scar, identified as Eb1 in figure 4a. Presently, the exact surface area and volume of Eb1 is unclear, as the volume loss exceeds the coverage of the 2023 ALS dataset. However, a preliminary estimate has been attempted, resulting in a minimum volume of 58,000 m^3. The failure was documented on photographs in the immediate aftermath of the event by passers-by (Fig. 4b).

The area involved in the failure depicted in the photograph seems smaller compared to the area affected by volume loss in the change detection analysis results, suggesting that another major failure affected this sector of the failure surface or, alternatively, a colluvial deposit upslope of the failed block mobilized after and as a result of the failure.

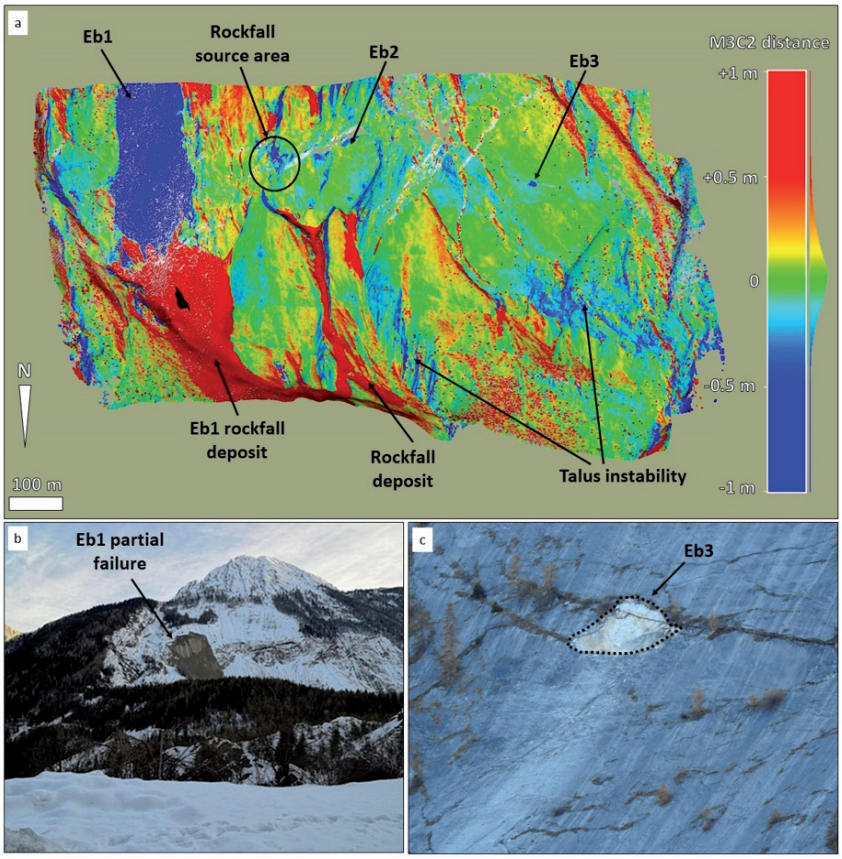

Fig. 4 - Overview of the results of the ALS change detection of the eastern lobe. Red and blue colors indicate gain and loss of material. Colorscale has been trimmed at negative and positive changes of 1 m. a) General view of the investigated area. Note the major loss of material from the eastern part of the slope. b) photograph of the 2021 rockfall that contributed to the loss of material identified as Eb1 in tab a (photo courtesy of Piero Gianolla). c) detail of the area where block Eb3 has been identified. This appears to be a relatively recent event, in view of the low alteration of the detachment surface

In general, widespread rockfall appears to have characterized the eastern lobe. In some cases, it is a simple task to identify missing blocks through the change detection analysis, as in the case of blocks Eb2 (surface area of 158 m^2 and estimated volume of 50 m^3) and Eb3 (surface area of 67 m^2 and estimated volume of 35 m^3) (Fig. 4). In other places, however, widespread volume loss marks the presence of large rockfall source areas that make the identification of the detachment surfaces of single rockfall events extremely challenging. In such cases, a visual inspection of surface alteration may provide indications on the relative timing of various rockfalls. To this aim, future studies will be undertaken exploiting a combination of visual analyses, multispectral imaging, and laser scanning.

All the rockfall blocks identified through the change detection analysis, perhaps with the exception of Eb1, are characterized by a tabular shape, and intuitively failed through a planar sliding mechanism along the bedding planes of the Fonzaso Formation, which are characterized by a spacing of 5-10 cm in the landslide area (Ghirotti, 1994).

The roughness of the basal failure surface is a significant controlling factor on the detachment of these types of rockfalls. During past fieldwork at the site, it was possible in places to observe tabular blocks lying on the planar basal surface (i.e., along low angle sections of the 1963 Vajont Slide failure surface), but physically separated from the slope along all sides (fig. 5). However, as the steepness of the basal surface increases, the role of frictional resistance reduces, and progressive damage and fracture propagation become more important.

In general, it is commonly accepted that brittle damage occurs in high stress environments, which result in the tensile/shear failure of intact rock. In fact, brittle damage due to fracture propagation is observed in conditions where stress levels are relatively low, such as at the surface of rock slopes. In the absence of brittle fracture propagation resulting in failure of in-plane and out-of-plane intact rock bridges, rockfall activity along steep rock slopes would be significantly lower. Across the sliding surface of the Vajont Slide, several examples of blocks that have detached due to brittle fracture propagation (i.e., failure of rock bridges)

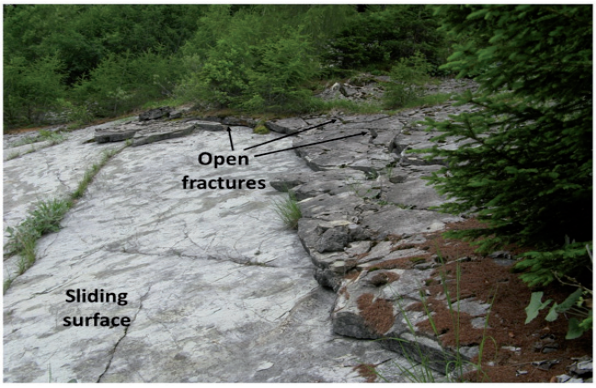

Fig. 5 - An area where tabular blocks lying on the sliding surface appear to be already detached on all sides (photograph courtesy of Andrea Wolter)

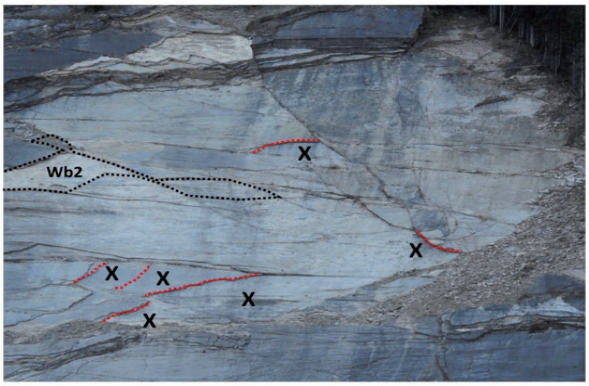

Fig. 6 - Examples of inferred brittle fracture features (red dashed lines) observed in the eastern lobe (Wb2 outline is included for reference). Black Xs represent the estimated location of blocks that detached following brittle fracturing of intact rock

can be noted (fig. 6), as well as blocks that are presently stable due to the presence of rock bridges that limit their kinematic freedom and removability. The combination of brittle damage accumulation and coalescence with pre-existing discontinuities is a critical factor controlling the evolution of rockfalls.

One of the challenges of investigating the evolution of a rock slope with time, and the estimation of volume of material involved in rockfall events, is related to the frequency at which surveys are performed. On the one hand, the collection of new ALS dataset at a relatively high frequency has the major challenge of data management, storage, and analysis capability. On the other hand, the ability to associate volume losses to multiple smaller rockfalls rather than single larger events is greatly enhanced. Williams *et alii* (2018) monitored the progressive detachment of rockfalls from a coastal cliff in UK in 1-hour intervals for over ten months, noting that the great majority (98%) of volume loss from the cliff was due to small rockfall events with volume lower than 0.1 m^3. By decreasing the scanning frequency (one month between subsequent surveys), this percentage decreases to 67%, resulting in a significant overestimation of the volume of single rockfalls. While the approach described by Williams *et alii* (2018) is a rigorous research application, not routinely applicable in common practice, it demonstrates that the ability of analyzing and interpretating the behavior and stability of rock slopes affected by rockfalls is strongly correlated with the type and frequency of monitoring.

At the Vajont Slide site, the volume estimation of single rockfalls that can be performed (of which a preliminary example has been described in this study) is likely skewed by the six-year-long interval between the ALS surveys (2017-2023). This is also exemplified in figure 7, which shows photographs of the rockfall identified as Wb2. While the change detection analysis allowed for the volume of material loss to be estimated at 105 m^3, a pre-failure photograph, collected during a field survey in 2010, showed that the loss volume was possibly composed of up to eight smaller blocks, separated by discontinuities. In this sense, the important role of internal boundaries and release surfaces on the behavior, stability, and size of rockfalls is emphasized. In the absence of high-resolution photographs of the area between 2010 and 2023, it remains unclear the number of events that ultimately resulted in the estimated volume loss.

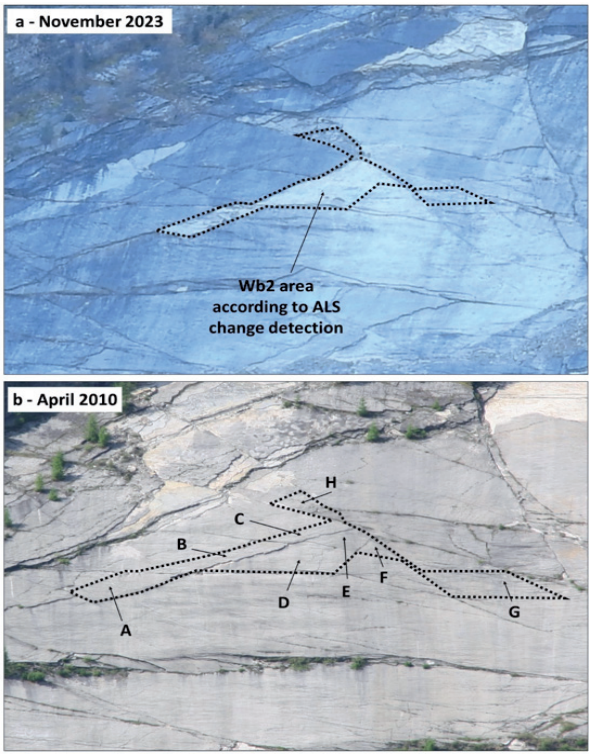

Fig. 7 - Challenge in defining the volume of rockfall events with longer survey frequency. a: area affected by volume loss as observed in the ALS change detection analysis. b) the same area in a photograph collected in 2010, showing that the loss volume was divided in multiple blocks by discontinuities acting as internal boundaries and release surfaces (photograph courtesy of Andrea Wolter)

FINAL REMARKS

This paper presented a preliminary, multi-temporal geomorphological analysis of the sliding surface of the 1963 Vajont Slide. The results described represent the initial step of a research aiming at the investigation of the residual, post-failure stability and behavior of rock slopes affected by major landslides, and the role played by stress redistribution and kinematics on the progressive accumulation of damage. In this sense, the Vajont Slide site represents an ideal research site, in view of the significant activity that has characterized the slope surface since the occurrence of the 1963 catastrophic event, and the absence of remediation measures that would limit or prevent further, localized, small-scale instability.

The study is based on a change detection analysis that has been performed using a pair of ALS datasets collected in 2017 and 2023, together with high-resolution photographs collected in the course of various fieldworks and activities conducted by the authors at the site. At this time, the investigation has been limited to two areas, located on the western and eastern lobes of the outcropping failure surface of the 1963 landslide.

In the western lobe, rockfall activity largely involved tabular blocks, with limited thickness controlled by bedding spacing, that displaced through a planar sliding mechanism. In the eastern lobe, local instability events are generally characterized by a more significant volume as evidenced by the detachment of a large block in February 2021 (minimum estimated volume of 58,000 m^3). Another major detachment, occurred sometimes between 2009 and 2011, is currently under investigation, and has not been treated here.

The next phase of the research will include a UAV-ALS survey of the whole area of the deposit and outcropping failure surface, and a landslide-scale change detection analysis using the LiDAR dataset collected in 2017 and an older one surveyed in 2010. The multi-temporal analysis 3D analysis will be combined with a 2D analysis that will take advantage of sets of photographs taken by the authors over the past thirty years, as well as recent and historical photographs that have been released and made available over the years. By combining change detection analyses (exploiting both ALS datasets and SfM models created using historical aerial imagery) with visual assessment of RGB imagery, we aim at reconstructing in detail the evolution of the slope over the past sixty year, as well as highlighting the most important factor controlling the post-failure evolution of rock slopes affected by major landslides.

REFERENCES

Brodu N. & Lague D. (2012) - *3D terrestrial lidar data classification of complex natural scenes using a multi-scale dimensionality criterion: applications in geomorphology.* ISPRS Journal of Photogrammetry and Remote Sensing, **68**: 121 34. https://doi.org/10.1016/j.isprsjprs.2012.01.006.

CloudCompare (2022) - *CloudCompare 2.12 [GPL Software].* Available at: https://www.cloudcompare.org/. Accessed on: January 1st, 2024.

DJI (2023a) - *DJI Pilot 2*. Available at: https://www.dji.com/. Accessed on: January 1st, 2024.

DJI (2023b) - *DJI Terra*. Available at: https://enterprise.dji.com/it/dji-terra. Accessed on: January 1st, 2024.

Donati D., Stead D. & Borgatti L. (2023) - *The importance of rock mass damage in the kinematics of landslides.* Geosciences, **13**(2): 52.

Friele P., Millard T.H., Mitchell A., Allstadt K.E., Menounos B., Geertsema M. & Clague J.J. (2020) - *Observations on the May 2019 Joffre Peak Landslides, British Columbia.* Landslides, **17**(4): 913-930.

Ghirotti M. (1994) - *Modellazione numerica della frana del Vajont sulla base di nuovi dati*. Geologica Romana, **30**: 207-216.

Ghirotti M. (2012) - *The 1963 Vaiont Landslide, Italy*. In: Stead. D. & Clague J.J. (2012, eds.) - *Landslides: Types, Mechanisms and Modeling*: 359-372. Cambridge University Press, Cambridge, UK.

Giudici F. & Semenza E. (1960) - *Studio geologico sul serbatoio del Vajont.* Unpublished technical report for Società Adriatica di Elettricità, Venice, Italy (in Italian).

Hendron A.J. & Patton F.D. (1987) - *The Vaiont Slide - A geotechnical analysis based on new geologic observations of the failure surface*. Engineering Geology, **24**(1–4): 475-491.

Kromer R.A., Hutchinson D.J., Lato M.J., Gauthier D. & Edwards T. (2015) - *Identifying Rock Slope Failure Precursors Using LiDAR for Transportation Corridor Hazard Management.* Engineering Geology, **195**: 93-103.

Lague D., Brodu N. & Leroux J. (2013) - *Accurate 3D comparison of complex topography with terrestrial laser scanner: application to the Rangitikei Canyon (N-Z)*. ISPRS Journal of Photogrammetry and Remote Sensing, **82**: 10-26.

Massironi M., Zampieri D., Superchi L., Bistacchi A., Ravagnan R., Bergamo A., Ghirotti M. & Genevois R. (2013) - *Geological structures of the Vajont Landslide*. Italian Journal of Engineering Geology and Environment, Special Issue: The 1963 Vajont Landslide (Northeast Alps, Italy): 573-582.

Paronuzzi P. & Bolla A. (2012) - *The prehistoric Vajont rockslide: an updated geological model.* Geomorphology, **169–170:** 165 191.

Rosser N.J., Lim M., Petley D., Dunning S. & Allison R. (2007) - *Patterns of precursory rockfall prior to slope failure*. J. Geophys. Res., **112**: F04014.

Semenza E. & Ghirotti M. (2000) - *History of the 1963 Vaiont Slide: the importance of geological factors*. Bulletin of Engineering Geology and the Environment, **59**(2): 87-97.

Semenza E. (1965) - *Sintesi degli studi geologici sulla frana del Vaiont dal 1959 al 1964.* Memorie Del Museo Tridentino Di Scienze Naturali, **16**(I): 1-52.

Walton G., Christiansen C., Kromer R. & Silaev A. (2023) - *Evaluation of rockfall trends at a sedimentary rock cut near Manitou Springs, Colorado,*

Using Daily Photogrammetric Monitoring. Landslides, **20**(12): 2657-2674.

Willenberg H., Loew S., Eberhardt E., Evans K.F., Spillmann T., Heincke B., Maurer H. & Green A.G. (2008) - *Internal structure and deformation of an unstable crystalline rock mass above Randa (Switzerland): Part I - internal structure from integrated geological and geophysical investigations.* Engineering Geology, **101**(1–2): 1 14.

Williams, J.G., Rosser, N.J., Hardy, R.J., Brain, M.J. & Afana, A.A. (2018) - *Optimising 4-D surface change detection: an approach for capturing rock-fall magnitude–frequency.* Earth Surface Dynamics, **6**(1): 101-119.

Wolter A., Stead D., Ward B.C., Clague J.J. & Ghirotti M. (2016) - *Engineering geomorphological characterisation of the Vajont Slide, Italy, and a new interpretation of the chronology and evolution of the landslide.* Landslides, **13**(5): 1067 1081.

Wyllie d. (2017) - *Rock Slope Engineering.* 5th ed. Taylor & Francis, CRC Press, Boca Raton, FL, USA.

Received January 2024 - Accepted March 2024